



Cite this: *Soft Matter*, 2018, 14, 4081

Received 30th January 2018,
 Accepted 16th February 2018

DOI: 10.1039/c8sm00226f

rsc.li/soft-matter-journal

Efficient simulation method for nano-patterned charged surfaces in an electrolyte solution

Amin Bakhshandeh,^{id}^a Alexandre P. dos Santos^{ab} and Yan Levin^{id}^{*a}

We present a method to efficiently simulate nano-patterned charged surfaces inside an electrolyte solution. Simulations are performed in the grand canonical ensemble and are used to calculate the force between surfaces with various charge patterns. The electric field produced by the surfaces is calculated analytically and is used as an external potential. To treat the long range Coulomb interaction between the ions we use a modified 3d Ewald summation method. The force between the surfaces is found to depend strongly on the specific charge pattern, on the surface alignment and separation.

1. Introduction

Electrostatic interactions between ions and macromolecules are responsible for many important phenomena in physics, chemistry, and biology.¹ In aqueous suspensions, ions screen repulsive interactions between colloidal particles leading to precipitation at sufficiently large concentrations of electrolyte. Presence of multivalent counterions can also result in charge reversal and attraction between like-charged macromolecules.^{2–5} Multivalent counterions at sufficiently large concentrations can lead to condensation of DNA into toroidal bundles, which are of fundamental importance for packing DNA in bacteriophages.^{6,7} For weakly charged surfaces and electrolyte solutions containing exclusively monovalent ions, mean-field theories have proven to be very successful in elucidating the underlying physics. The Derjaguin–Landau–Verwey–Overbeek (DLVO) theory,^{8,9} for example, provides a qualitative picture of stability of colloidal suspensions with 1 : 1 electrolyte, but is not sufficient to explain the specific ion (Hofmeister effect) or to elucidate the mechanism responsible for the stability of colloidal suspensions with multivalent electrolytes.^{10–12} For these reasons, computer simulation is still the most reliable way to obtain quantitative understanding of systems in which Coulomb interaction plays the dominant role.

Many important physicochemical systems contain surfaces with charged domains. Recent nano-fabrication techniques allow creation of periodically charged patterned surfaces for application in nanotechnology.^{13,14} In biology, proteins can

adsorb to the outer layer of cell membranes resulting in charged domains.¹⁵ Much attention has been devoted to the study of heterogeneously charged surfaces^{16–21} in electrolyte solutions for which long ranged attraction was observed.^{22–27} Interaction between DNA and nano-patterned surfaces²⁸ has also attracted a lot of attention due to possible technological applications. One of the important parameters for periodically modulated surfaces is the effective Debye–Hückel decay length, which plays an important role in the interactions between periodically patterned helices, and also of symmetric distribution of charges on spheres.^{29,30} Simulations of electrostatic systems is very difficult because the long-range Coulomb force precludes use of simple periodic boundary condition. Instead the whole system must be periodically replicated with a suitable symmetry. Summation over the replicas can be performed using Ewald techniques. If the electrolyte is confined between the nano-patterned charged surfaces one can include the surface charges in the Ewald summation.²⁰ This, however, will significantly slow down simulations, since to obtain an accurate description of a continuous surface charge distribution will require a huge number of surface point charges, which will have to be included in the Ewald sum. Clearly a more efficient approach would be to separate the electrostatic potential produced by the periodic surface charge distribution, which can be calculated analytically, from the potential produced by the ions. The difficulty is to combine this with the Ewald treatment of the whole system. In the present paper, we will introduce a method which allows us to efficiently simulate interactions between nano-patterned surfaces. To this end we will consider surfaces with periodic sinusoidal charge density. Analytical solution of the Poisson equation allows us to explicitly calculate the electrostatic potential produced by such surfaces. This potential can then be used as a external field in the Grand Canonical Monte Carlo (GCMC) simulations. The long range

^a Instituto de Física, Universidade Federal do Rio Grande do Sul, Caixa Postal 15051, CEP 91501-970, Porto Alegre, RS, Brazil.
 E-mail: amin.bakhshandeh@ufrgs.br, alexandre.pereira@ufrgs.br, levin@if.ufrgs.br

^b Fachbereich Physik, Freie Universität Berlin, 14195 Berlin, Germany

Coulomb interactions between the ions can be treated using recently developed modified 3d Ewald summation method.³¹

The balance of the paper is as follows. In Section II, we explain the model and analytical calculations. The simulation details are considered in Section III. Results are shown in Section IV and conclusions are presented in Section V.

II. Electrostatic potential between the nano-patterned surfaces

Consider an infinite surface located at $z = 0$, carrying a periodic charge density

$$\sigma(x,y) = \sigma_0 \sin(k_x x + \varphi_x) \sin(k_y y + \varphi_y), \quad (1)$$

where σ_0 is the amplitude, $\varphi_{x,y}$ phases, $k_x = 2\pi n_x/L_x$, $k_y = 2\pi n_y/L_y$, with L_x and L_y periods of charge density oscillations in x and y directions, respectively, and $n_{x,y}$ are integers. Using the sinusoidal charge distribution we can create different charge patterns on the surfaces by varying k_x and k_y . In the present work we will consider 4 possibilities depicted in Fig. 1. The electrostatic potential produced by the surface charge density of eqn (1) can be obtained from the solution of Laplace equation,

$$\nabla^2 \Phi(\mathbf{r}) = 0. \quad (2)$$

The potential must vanish in the limit $z \rightarrow \pm\infty$, yielding a general solution

$$\Phi(\mathbf{r}) = A_1 \sin(k_x x + \varphi_x) \sin(k_y y + \varphi_y) e^{-\alpha|z|}, \quad (3)$$

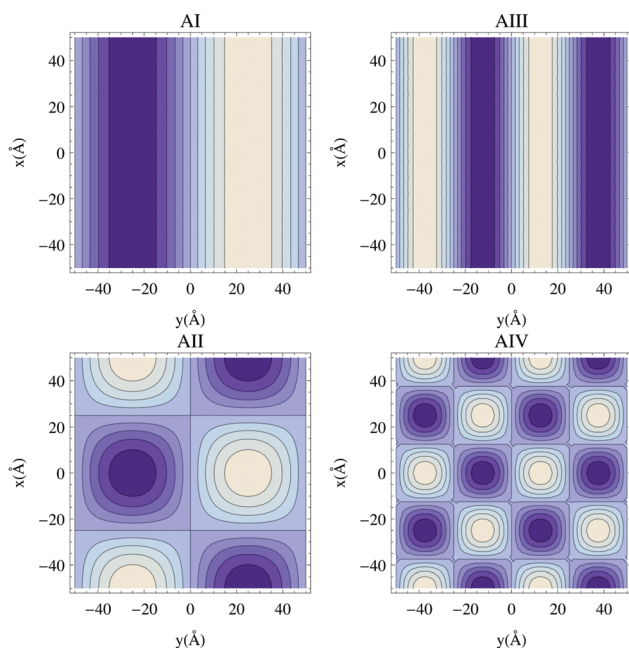


Fig. 1 Different charge patterns explored in the present study with $L_x = L_y = 400$ Å. (AI) $n_x = 4$, $n_y = 0$, (AII) $n_x = 4$, $n_y = 4$, (AIII) $n_x = 8$, $n_y = 0$, and (AIV) $n_x = 8$, $n_y = 8$. Dark and light regions represent opposite charges. The phases are set to $\varphi_x = 0$ and $\varphi_y = \pi/2$. The plots are limited from -50 Å to 50 Å.

where

$$\alpha(k_x, k_y) = \sqrt{k_x^2 + k_y^2}. \quad (4)$$

The amplitude of the electrostatic potential, A_1 , can be obtained using the boundary condition at $z = 0$,

$$(\mathbf{E}_{z>} - \mathbf{E}_{z<}) \cdot \mathbf{n} = \frac{4\pi\sigma(x,y)}{\epsilon_w}, \quad (5)$$

where $\mathbf{E}_{z>}$ and $\mathbf{E}_{z<}$ are the electric fields in the regions $z > 0$ and $z < 0$, respectively, and \mathbf{n} is the normal vector pointing in $z > 0$ direction. Using eqn (3) we obtain

$$A_1 = \frac{2\pi\sigma_0}{\epsilon_w \alpha(k_x, k_y)}. \quad (6)$$

If there are two charge patterned surfaces located at $z = -d/2$ and $z = d/2$, the electrostatic potential can be found using superposition:

$$\Phi(\mathbf{r}) = \frac{2\pi\sigma_0}{\epsilon_w} \left[\frac{\sin(k_x^a x + \varphi_x^a) \sin(k_y^a y + \varphi_y^a) e^{-\alpha(k_x^a, k_y^a)|z+d/2|}}{\alpha(k_x^a, k_y^a)} + \frac{\sin(k_x^b x + \varphi_x^b) \sin(k_y^b y + \varphi_y^b) e^{-\alpha(k_x^b, k_y^b)|z-d/2|}}{\alpha(k_x^b, k_y^b)} \right], \quad (7)$$

where superscripts a and b refer to the first and second surfaces, respectively. In the current study we will use $\varphi_x^a = 0$, $\varphi_x^b = 0$, and $\varphi_y^a = \varphi_y^b = \pi/2$ for symmetric surfaces—when like charged domains are opposite of each other—and $\varphi_x^b = \pi$ for antisymmetric case, when the oppositely charged domains are opposite of each other.

To perform computer simulations of systems with Coulomb interactions requires a particular care. The long range nature of the Coulomb force precludes one from using simple periodic boundary conditions. Instead, the simulation box must be periodically replicated, so that the ions in the main simulation cell interact both with real ions and with their periodic replicas. In the absence of interfaces the sum over the replicas can be efficiently performed using Ewald summation methods. For systems with slab geometry, such as electrolyte confined between two surfaces, there are additional complications related with the reduced symmetry. These can be overcome using a modified 3d Ewald summation method which accounts for the conditional convergence of the lattice sum, and by introducing a sufficiently large vacuum region devoid of any charge.³¹ Nevertheless, presence of transverse replicas can lead to some undesired artifacts. Therefore, we first test that our analytical expression agrees with the electrostatic potential produced by point charges distributed according to eqn (1) with $n_x = 1$ and $n_y = 0$ and replicated using modified Ewald summation method.³¹ The charge of each point particle is adjusted so that the net charge within a given domain is the same as for the continuous distribution. In Fig. 2 we compare the potential difference $\Delta\phi(z) = \phi(z) - \phi(0)$ at $x = L_x/4$ and $y = L_y/4$ calculated using the exact electrostatic potential with the one obtained using Ewald summation method. As the number of

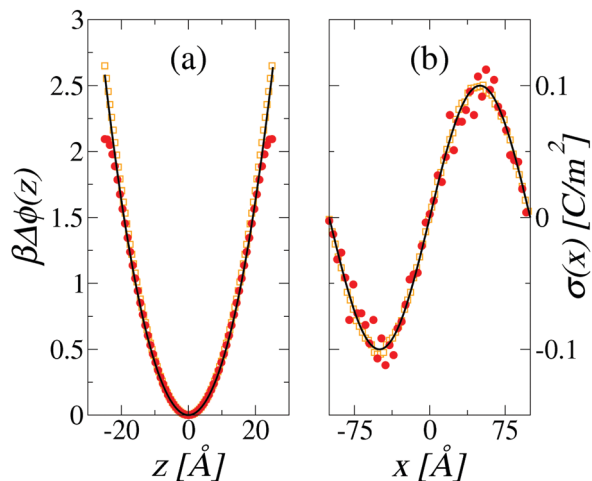


Fig. 2 (a) Electrostatic potential difference between the symmetric surfaces with $n_x = 1$, $n_y = 0$ and $L_x = L_y = 200$ Å, as a function of z , along the line located at $x = L_x/4$, $y = L_y/4$ and parallel to the z axis. The separation between the surfaces is $d = 50$ Å and amplitude of the surface charge is $\sigma_0 = 0.1$ C m⁻². Solid line is the analytical expression, eqn (7), and symbols are the result of numerical calculation using a modified Ewald summation with different number of point charges N : circles $N = 1000$ and squares $N = 40\,000$. (b) Surface charge distribution for different number of point charges compared to the analytical expression, eqn (1).

point charges on each surface increases, the electrostatic potential difference converges to the exact analytical result.

III. Simulation method

We are now in a position to study interaction between two parallel nano-patterned charged surfaces inside an electrolyte solution. The two surfaces have dimensions L_x and L_y and are separated by a distance d . We set $L_x = L_y = 400$ Å and $\sigma_0 = 0.05$ C m⁻² for all results, except Fig. 2 and 3. The confined electrolyte is considered within the primitive model, cations and anions are represented by spheres of radius 2 Å with the charge $\pm q$ at their centers, where q is the proton charge. The number of ions in between the surfaces is determined by the reservoir salt concentration which we set at $\rho_s = 50$ mM. The solvent is assumed to be structureless, with a uniform dielectric of permittivity ϵ_w . The Bjerrum length, defined as $\lambda_B = q^2/\epsilon_w k_B T$, is 7.2 Å, value for water at room temperature. The whole system is replicated infinitely in the x and y directions.

To perform the simulations we use a GCMC algorithm.^{32–34} In order to keep the charge neutrality, if a cation of valence α is added or removed from a system, α anions must also be added or removed.³⁴ The total electrostatic energy is given by:^{31,35–37}

$$\begin{aligned}
 U = & \sum_{\mathbf{k} \neq 0} \frac{2\pi}{\epsilon_w V |\mathbf{k}|^2} \exp\left[-\frac{|\mathbf{k}|^2}{4\kappa_c^2}\right] [A(\mathbf{k})^2 + B(\mathbf{k})^2] \\
 & + \frac{2\pi}{\epsilon_w V} [M_z^2 - Q_z G_z] + \frac{1}{2} \sum_{i \neq j}^N q_i q_j \frac{\text{erfc}(\kappa_c |\mathbf{r}_i - \mathbf{r}_j|)}{\epsilon_w |\mathbf{r}_i - \mathbf{r}_j|} \\
 & + \sum_{i=1}^N q_i \Phi(\mathbf{r}_i),
 \end{aligned} \quad (8)$$

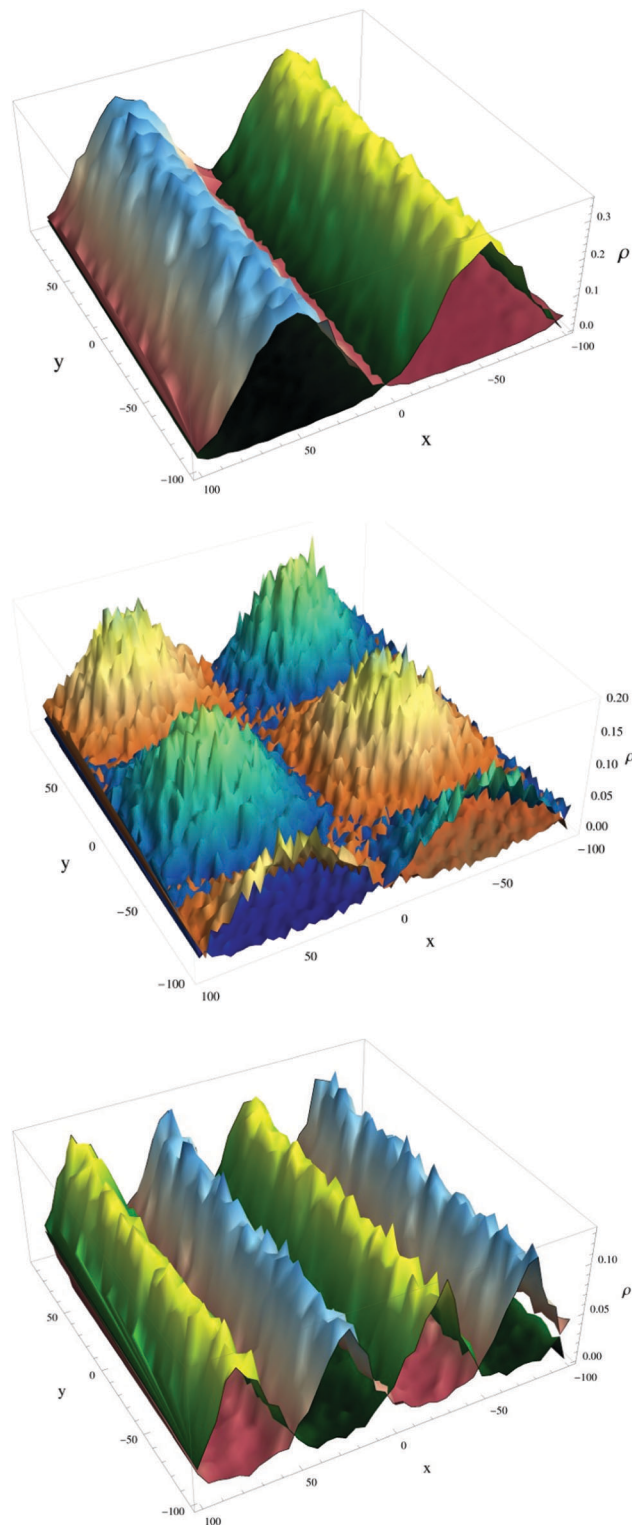


Fig. 3 Density of positive and negative ions in a bin $\Delta z = 3$ Å at contact for ($n_x = 1$ and $n_y = 0$), ($n_x = 1$ and $n_y = 1$) and ($n_x = 2$ and $n_y = 0$), from top to bottom, respectively. The charge density is $\sigma = 0.1$ C m⁻² while simulation box length is $L_x = L_y = 200$ Å and $d = 15$ Å. x and y axis are in units Å and density (ρ) in M. Darker and lighter colors represent positive and negative ions, respectively.

where

$$\begin{aligned}
 A(\mathbf{k}) &= \sum_{i=1}^N q_i \cos(\mathbf{k} \cdot \mathbf{r}_i), \\
 B(\mathbf{k}) &= -\sum_{i=1}^N q_i \sin(\mathbf{k} \cdot \mathbf{r}_i), \\
 M_z &= \sum_{i=1}^N q_i z_i, \\
 G_z &= \sum_{i=1}^N q_i z_i^2 \quad \text{and} \quad Q_t = \sum_{i=1}^N q_i.
 \end{aligned}
 \tag{9}$$

The volume $V = L_x L_y L_z$ includes the vacuum region of the modified Ewald method where $L_z = 2L_x$. The damping parameter is $\kappa_e = 5/L_x$ while the k -vectors are $\mathbf{k} = (2\pi w_x/L_x, 2\pi w_y/L_y, 2\pi w_z/L_z)$ where w 's are integers. The electrostatic potential produced by the nano-patterned surfaces is introduced as an external field acting on the ions, see eqn (7). The equilibration is achieved with 10^5 MC steps, after which 10^5 uncorrelated particles configurations are saved for further analysis each 10^3 MC steps.

The pressure on the surfaces is calculated by taking into account the direct electrostatic interactions between surfaces and ions, as well as the entropic force arising from the momentum transfer during the collisions of the ions with the surfaces.^{38,39} The entropic contribution is obtained using the method of Wu *et al.*⁴⁰ The total pressure can be written as:

$$P = P_{ss} + P_{si} + P_{ent} - P_{res}, \tag{10}$$

where P_{ss} is the electrostatic contribution from the surface–surface interaction, P_{si} is due to electrostatic surface–ion interaction, P_{ent} is the entropic pressure and P_{res} is the pressure from the external reservoir which is obtained using separate *NPT* MC simulations.²⁰ The repulsive (positive) entropic pressure is given by:

$$\beta P_{ent} = \frac{\langle N_o \rangle}{\Delta z L_x L_y}, \tag{11}$$

where N_o is the number of overlaps of the wall with the free ions (which are held fixed) after a surface displacement Δz . The force is extrapolated to the value in which $\Delta z \rightarrow 0$. More details about the entropic and reservoir contributions can be found in ref. 20.

Here we simplify our system by setting $k_x^a = k_x^b = k_x$ and $k_y^a = k_y^b = k_y$, which means that surfaces carry identical, but not necessarily aligned charge distributions. We also consider, without loss of generality, $L_x = L_y = L$. Below we give the expressions for P_{ss} and P_{si} ,

$$P_{ss} = \frac{\pi\sigma_0^2 e^{-2(k_x, k_y)d}}{2\epsilon_w} \cos(\varphi_x^a - \varphi_x^b) \cos(\varphi_y^a - \varphi_y^b) \tag{12}$$

and

$$\begin{aligned}
 P_{si} &= \left\langle \sum_{i=1}^N q_i \frac{2\pi\sigma_0 e^{-\alpha(k_x, k_y)(d/2+z_i)}}{L^2 \epsilon_w} \right. \\
 &\quad \left. \times \sin(\varphi_x^a + k_x x_i) \sin(\varphi_y^a + k_y y_i) \right\rangle.
 \end{aligned}
 \tag{13}$$

The average is performed over the saved MC states.

IV. Results

We begin by calculating the ionic density profiles for systems with box sizes $L = 200 \text{ \AA}$ and $d = 15 \text{ \AA}$ with charge patterns $(n_x = 1, n_y = 0)$, $(n_x = 1, n_y = 1)$ and $(n_x = 2, n_y = 0)$, in a bin of length 3 \AA at the surface contact, see Fig. 3. The different colors indicate the positive and negative ions. The pressures, as a function of surface separation, for different charge patterns are shown in Fig. 4. The circles and triangles represent the symmetric and antisymmetric cases, respectively. The surface charge patterns are characterized by $\varphi_x^a = 0$, $\varphi_y^a = \varphi_y^b = \pi/2$ and $\varphi_x^b = 0$ for the symmetric cases and $\varphi_x^b = \pi$ for antisymmetric ones. In the symmetric case, surfaces are identical with the like-charged domains opposite of each other. We expect that in this case the pressure will be positive, and the surfaces will repel. In the antisymmetric case, where oppositely charged domains are aligned, we expect that the pressure will be negative, and the surfaces will attract. This is indeed what is found in simulations. As the number of charged domains increases, we observe that the absolute pressure decreases. This is in agreement with the previous simulations for heterogeneously charged surfaces.²⁰ If we compare the symmetric and antisymmetric arrangements, the modulus of pressure P is not the same for these configurations. In the symmetric case, for small (n_x, n_y) , there is a strong entropic contribution to the repulsive pressure, since counterions are driven into the region between the charged domains in order to neutralize the surface charge. The resulting collisions between the ions and the surfaces lead to a positive contribution to the osmotic pressure. On the other hand, for antisymmetric surfaces the local charge neutrality between oppositely

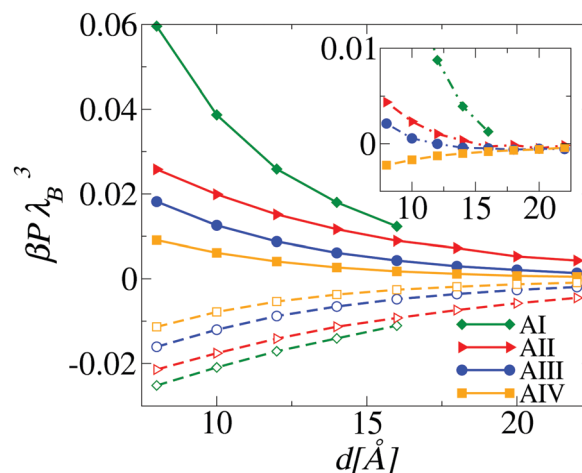


Fig. 4 Osmotic pressures for symmetric (full symbols and solid lines) and antisymmetric (empty symbols and dashed lines) surface arrangements carrying charge patterns (AI, AII, AIII and AIV): diamonds, triangles, circles and squares symbols, respectively. Symbols represent simulation data while lines are guides to the eye. In symmetric arrangement like charged regions of both surfaces are in front of each other (pressure is positive); in antisymmetric arrangement oppositely charged domains face each other (pressure is negative). The inset shows the sum of symmetric and antisymmetric cases. Note the change of behavior for (AIV) configuration, the modulus of pressure for antisymmetric alignment becomes larger than for the symmetric alignment.

charged domains is automatically satisfied even without any ions, diminishing ionic concentration in the gap and the amount of momentum transfer between ions and the surfaces. This observation explains why the net repulsion between symmetric surfaces with large patches is larger than the net attraction between the antisymmetric surfaces. For small charged domains (large n_x, n_y values), the entropic contribution of trapped ions diminishes and we find that the modulus of the attractive interaction between the antisymmetric surfaces becomes larger than the repulsive force for the symmetric surfaces, see inset of Fig. 4 which shows the sum of pressures for symmetric and antisymmetric arrangement with the same charge pattern. We also observe that for sufficiently large distances pressure decays exponentially with the separation between the surfaces, Fig. 5. For $\alpha:1$ electrolyte at bulk concentration ρ_s , we expect the decay to depend on the effective Debye length which can be calculated from the linearized Poisson–Boltzmann equation,

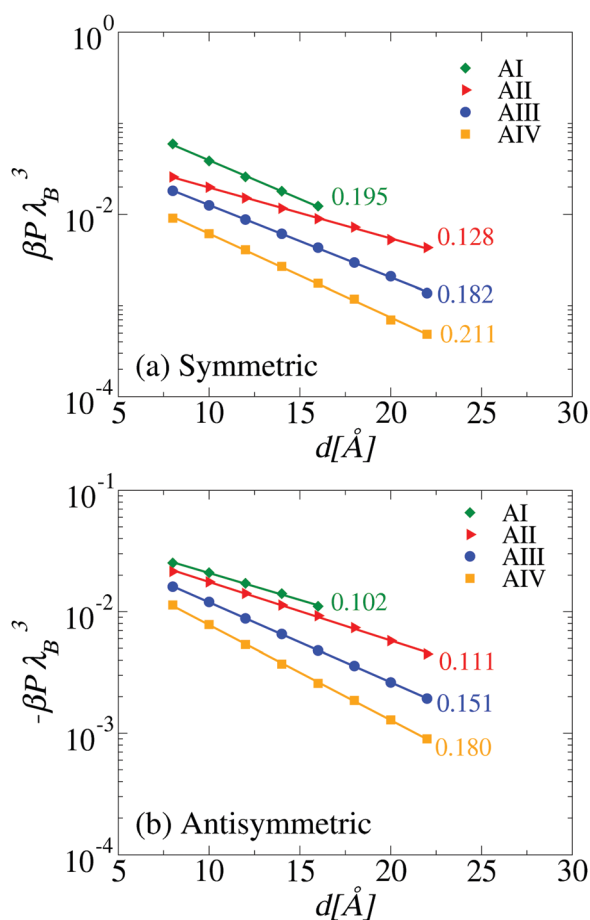


Fig. 5 Osmotic pressures for symmetric (a) and antisymmetric (b) surface arrangements carrying charge patterns (AI, AII, AIII, and AIV): diamonds, triangles, circles and squares symbols, respectively. Symbols represent simulation data while lines are exponential fitting. In symmetric arrangement like charged regions of both surfaces are in front of each other (pressure is positive); in antisymmetric arrangement oppositely charged domains face each other (pressure is negative). The fitting exponents are indicated in figure in units of \AA^{-1} . The theoretical values of κ_{eff} are: 0.096, 0.115, 0.145 and 0.192 \AA^{-1} for (AI, AII, AIII and AIV), respectively.

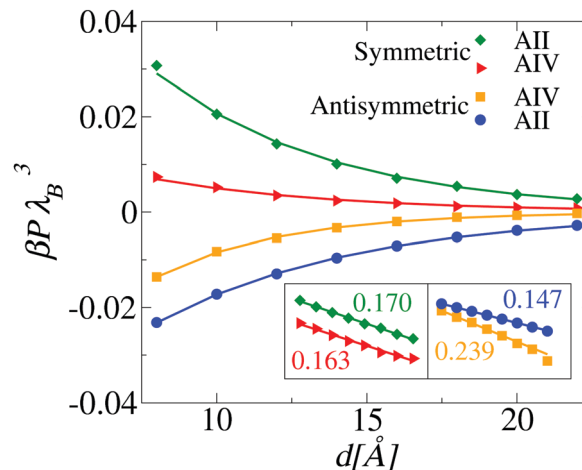


Fig. 6 Osmotic pressures in the presence of 2:1 salt for symmetric and antisymmetric configurations. Symbols represent simulation data while lines are exponential fitting. The diamonds and circles symbols represent (AII) charged pattern while triangles and squares represent (AIV). The fitting exponents are indicated in figure in units of \AA^{-1} . The theoretical values κ_{eff} are: 0.146 and 0.212 \AA^{-1} for (AII and AIV), respectively.

$\kappa_{\text{eff}} = \sqrt{k_x^2 + k_y^2 + \kappa^2}$, where the inverse Debye length is $\kappa = \sqrt{8\pi\lambda_B I}$, with the ionic strength $I = (\alpha^2\rho_s + \rho_s)/2$. We see, however, that for surface separations considered in the present study the linear Debye–Hückel equation is only qualitative, with the agreement much better for the antisymmetric alignment between the surfaces than for symmetric alignment. The agreement between theory and simulations is found to improve for larger values of (n_x, n_y) . Finally, we consider nano-patterned surfaces in a 2:1 electrolyte at 50 mM concentration, Fig. 6. Once again we see that pressure decays exponentially with separation between the surfaces. The decay rate is consistent with the linear theory, with antisymmetric alignment showing a much better agreement between the linear theory and simulations than symmetric alignment. The ionic charge asymmetry decreases the modulus of pressure and we see that similar to 1:1 electrolyte repulsion between symmetrically aligned surfaces with small (n_x, n_y) is larger than the attraction between antisymmetrically aligned surfaces. For larger values of (n_x, n_y) this behavior is reversed.

V. Conclusions

In this paper we have presented a simple and robust method for studying interactions between charged nano-patterned surfaces. We have focused on sinusoidal density distributions, however, the method can be easily extended to any arbitrary periodic charge distributions using Fourier series representation. The simulations were performed in the grand canonical ensemble. The osmotic pressure inside the reservoir was obtained using NPT simulations. However, for monovalent ions in aqueous electrolyte solutions one can use very accurate analytical expression for the pressure based on the mean spherical approximation (MSA). For the case of multivalent ions there are strong

electrostatic correlations and mean-field theories in general can not be used. The force between the surfaces was found to be very sensitive to the relative alignment between the charged domains and to the domain size. In all cases, for sufficiently large separations between the surfaces, the pressure was found to decay exponentially with distance. For antisymmetric alignment and large n_x or n_y (small charged domains) the decay length was found to be in a reasonably good agreement with κ_{eff} .

For now we have restricted our study to the overall charge neutral surfaces, however, the method introduced in this paper can also be extended to non-neutral surfaces with periodic charged domain. This will be the subject of future work.

Conflicts of interest

There are no conflicts to declare.

Acknowledgements

We dedicate this work to the memory of Per Linse who was a master of Coulomb systems simulations. The research was completed in part with computer resources provided by Instituto de Física e Matemática, Universidade Federal de Pelotas. This work was partially supported by CNPq, CAPES, Alexander von Humboldt Foundation, FAPERGS, INCT-FCx, and by the US-AFOSR under the grant FA9550-12-1-0438.

References

- 1 Y. Levin, *Rep. Prog. Phys.*, 2002, **65**, 1577.
- 2 P. Linse and V. Lobaskin, *Phys. Rev. Lett.*, 1999, **83**, 4208.
- 3 F. J. Solis and M. O. de la Cruz, *Phys. Today*, 2001, **54**, 71.
- 4 A. Naji and R. R. Netz, *Eur. Phys. J. E: Soft Matter Biol. Phys.*, 2004, **13**, 43.
- 5 S. Buyukdagli and T. Ala-Nissila, *J. Chem. Phys.*, 2017, **147**, 144901.
- 6 F. J. Solis and M. O. de la Cruz, *J. Chem. Phys.*, 2000, **112**, 2030.
- 7 V. D. Nguyen, T. T. Nguyen and P. Carloni, *J. Biol. Phys.*, 2017, **43**, 185.
- 8 B. V. Derjaguin and L. Landau, *Acta Physicochim. URSS*, 1941, **14**, 633.
- 9 E. J. W. Verwey and J. T. G. Overbeek, *Theory of the Stability of Lyophobic Colloids*, Elsevier, Amsterdam, 1948.
- 10 M. Peula-Garcia, J. L. Ortega-Vinuesa and D. Bastos-Gonzalez, *J. Phys. Chem. C*, 2010, **114**, 11133.
- 11 A. P. dos Santos and Y. Levin, *Phys. Rev. Lett.*, 2011, **106**, 167801.
- 12 C. Schneider, M. Hanisch, B. Wedel, A. Jusufi and M. Ballauff, *J. Colloid Interface Sci.*, 2011, **358**, 62.
- 13 R. Parthasarathy, P. A. Cripe and J. T. Groves, *Phys. Rev. Lett.*, 2005, **95**, 048101.
- 14 M. Sayin and R. Dahint, *Nanotechnology*, 2017, **28**, 135303.
- 15 A. R. Sapuri, M. M. Baksh and J. T. Groves, *Langmuir*, 2003, **19**, 1606.
- 16 S. J. Miklavic, D. Y. C. Chan, L. R. White and T. W. Healy, *J. Phys. Chem.*, 1994, **98**, 9022.
- 17 D. Velegol and P. K. Thwar, *Langmuir*, 2001, **17**, 7687.
- 18 C. C. Fleck and R. R. Netz, *Eur. Phys. J. E: Soft Matter Biol. Phys.*, 2007, **22**, 261.
- 19 Y. S. Velichko, F. J. Solis and M. O. de la Cruz, *J. Chem. Phys.*, 2008, **128**, 144706.
- 20 A. Bakhshandeh, A. P. dos Santos, A. Diehl and Y. Levin, *J. Chem. Phys.*, 2015, **142**, 194707.
- 21 J. M. Dempster and M. O. de la Cruz, *ACS Nano*, 2016, **10**, 5909.
- 22 E. E. Meyer, Q. Lin, T. Hassenkam, E. Oroudjev and J. N. Israelachvili, *Proc. Natl. Acad. Sci. U. S. A.*, 2005, **102**, 6839.
- 23 R. Podgornik and A. Naji, *Europhys. Lett.*, 2006, **74**, 712.
- 24 D. S. Dean, A. Naji and R. Podgornik, *Phys. Rev. E: Stat., Nonlinear, Soft Matter Phys.*, 2011, **83**, 011102.
- 25 G. Silbert, D. Ben-Yaakov, Y. Dror, S. Perkin, N. Kampf and J. Klein, *Phys. Rev. Lett.*, 2012, **109**, 168305.
- 26 D. Ben-Yaakov, D. Andelman and H. Diamant, *Phys. Rev. E: Stat., Nonlinear, Soft Matter Phys.*, 2013, **87**, 022402.
- 27 R. M. Adar, D. Andelman and H. Diamant, *Adv. Colloid Interface Sci.*, 2017, **247**, 198.
- 28 B. Teshome, S. Facsko and A. Keller, *Nanoscale*, 2014, **6**, 179.
- 29 A. A. Kornyshev, D. J. Lee, S. Leikin and A. Wynveen, *Rev. Mod. Phys.*, 2007, **79**, 943.
- 30 A. L. Bozic and R. Podgornik, *J. Chem. Phys.*, 2013, **138**, 074902.
- 31 A. P. dos Santos, M. Giroto and Y. Levin, *J. Chem. Phys.*, 2016, **144**, 144103.
- 32 J. P. Valleau and L. K. Cohen, *J. Chem. Phys.*, 1980, **72**, 5935.
- 33 D. Frenkel and B. Smith, *Understanding Molecular Simulation*, Academic Press, New York, 1996.
- 34 M. P. Allen and D. J. Tildesley, *Computer Simulations of Liquids*, Oxford University Press, Oxford, 1987.
- 35 I. C. Yeh and M. L. Berkowitz, *J. Chem. Phys.*, 1999, **111**, 3155.
- 36 Z. Hu, *J. Chem. Theory Comput.*, 2014, **10**, 5254.
- 37 S. Yi, C. Pan and Z. Hu, *J. Chem. Phys.*, 2017, **147**, 126101.
- 38 R. Podgornik, T. Kesson and B. Jönsson, *J. Chem. Phys.*, 1995, **102**, 9423.
- 39 E. Allahyarov, I. D'Amico and H. Lowen, *Phys. Rev. Lett.*, 1998, **81**, 1334.
- 40 J. Z. Wu, D. Bratko, H. W. Blanch and J. M. Prausnitz, *J. Chem. Phys.*, 1999, **111**, 7084.